Pramāṇa, Vol. 2, No. 4, 1974, pp 199–218. Printed in India.

Structure calculations in ^{18}O nucleus

J N DE and M K PAL
Saha Institute of Nuclear Physics, Calcutta 700009

MS received 8 September 1973; after revision 9 March 1974

Abstract. A multishell Hartree-Fock calculation for ^{18}O nucleus has been done with the Tabakin and Hamada-Johnston interactions followed by pairing correlations and angular momentum projection. The B(E2) transition rates have been reproduced with an effective charge of $1.5e$ for protons and $0.5e$ for neutrons, but the fit to energy levels is poor. An approximate alternative formalism has then been developed which casts the eighteen-particle problem into a two-valence nucleon problem. The two valence nucleons interact through the RPA-type oscillation modes of the core. Calculations with the two interactions mentioned above have reproduced roughly the uncorrelated projected Hartree-Fock spectrum. Lastly, the excited band spectra of ^{18}O have been examined in the TDA approach followed by band mixing.

Keywords. Oxygen-18 nucleus; nuclear structure; nuclear spectroscopy.

1. Introduction

For low-lying nuclear states, the ^{18}O nucleus may be simply viewed as an ^{16}O core with two valence nucleons confined to the s-d shell. The two-nucleon secular matrix is diagonalised within this limited subset of states to obtain the level spectrum. Following Brueckner's prescription, the free nucleon-nucleon interaction is replaced by the reaction matrix t (Brueckner 1955). Though it is smooth and well behaved, it is still too strong to confine the valence nucleons to the limited space, usually called the model space. A more straightforward way to have a better representation is to include more configurations in the calculation, but then computational difficulties increase rapidly. To include the effects of the states left out of the model space, a perturbative approach is followed which amounts to a renormalisation of the reaction matrix. This renormalised interaction between the valence nucleons is called the effective interaction G. The formal theory for evaluating the effective interaction matrix elements was given by Bloch and Horowitz (1958). They unlink the valence nucleons from the core and then allow interactions between the valence nucleons through core excitations to infinite orders of the perturbation theory. Formally, this is done by expanding G in a power series in the Brueckner-reaction matrix.

Kuo and Brown (1966) and then others (Kuo 1967, Clement and Baranger 1968) calculated matrix elements of G with realistic potentials (Hamada and Johnston

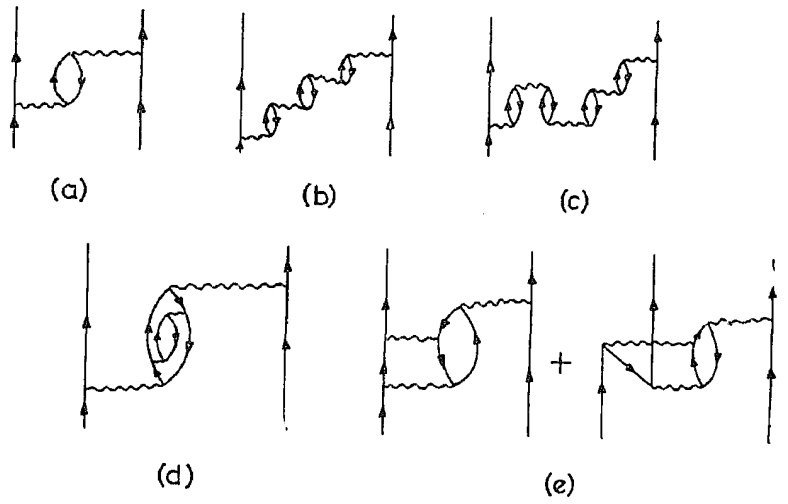

Figure 1. (*a*) The 3p–1h diagram; (*b*) The TDA diagram; (*c*) The RPA diagram; (*d*) Self screening; (*e*) Vertex-renormalisation.

1962, Tabakin 1964). They stopped at the second order. One of the second-order processes was found to be very important in bringing an impressive experimental fit of the level spectra. This process is shown diagrammatically in figure 1 *a*. Here one of the valence nucleons interacts with the core and then excites a nucleon from an occupied (hole) state to an unoccupied state (particle) just outside the model space. A particle-hole (p-h) pair is then formed; the excited particle then interacts with the other valence nucleon and goes back to its original state thus destroying the p-h pair. This particular diagram is known as core-polarisation diagram in the literature.

The second-order terms were found to be of the same order of magnitude as the first-order terms and to test the convergence of the perturbation series, Barrett and Kirson (1970) calculated all the third-order terms and a few selected fourth-order terms. They found that nearly all the third-order terms were of the same order of magnitude as the second-order terms. This particular feature does not allow much confidence in the low-order calculations and also throws doubt on the convergence of the perturbation expansion.

Selected sums of higher order diagrams in the perturbation theory were tried by various authors (Ellis and Siegel 1970, Kirson and Zamick 1970, Osnes *et al* 1971), such as the TDA or the RPA type particle-hole excitation, self-screening of the hole-particle interaction and vertex renormalisation. The results fluctuate widely. A way of summing up all the important terms to infinite orders was obtained by Kirson (1971) through a set of self-consistent equations to be solved in an iterative manner. The results are equally disturbing.

In all these calculations, it is assumed that the valence states as well as the core states are spherical harmonic oscillatior (HO) states. The valence states are allowed deformation through configuration-mixing (shell-model diagonalisation) and the core states are allowed partial deformation through particle-hole (p-h) excitations. It is well known that even without recourse to the renormalisation programme, effects of deformation can be included in a self-consistent Hartree-Fock (HF) theory provided the basis in which the single particle orbitals are expanded is large enough. We try to analyse the core polarisation problem in this alternative way. Through this procedure, not only the core states are allowed defor-

mation in every possible way, but also the valence states are allowed polarisation which in turn induces an extra polarisation of the core states.

The HF wavefunction is the zeroth order wave function in the Rayleigh-Schrödinger many-body perturbation theory. Perturbation corrections are built on the HF solution to give a better description of the core-polarisation phenomena. Finally, states of good angular momentum are projected out to compare the computed results with the experimental ones. This is a tedious and time-consuming job and it is difficult to apply this procedure directly to heavier nuclei. To explore core-polarisation for all two-valence nucleon systems in the periodic table, an alternative formalism has been presented in this paper, which is in essence an approximation scheme to the HF theory. In practice, the HF single-particle Hamiltonian is broken into a diagonal and a non-diagonal part, and perturbation corrections are built up corresponding to the perturbative nondiagonal field. Ultimately, the standard RPA matrix is met with, diagonalisation of which yields p-h excitation amplitudes, the mixing amplitudes of the p-h states to the unperturbed solution. Lastly, angular momentum projection is achieved from this mixture through simple decoupling and recoupling of angular momenta.

The H-J and Tabakin interactions are chosen as the basic two-nucleon potentials. The H-J matrix elements are evaluated with the standard Kuo-Brown prescription, mostly because of simplicity, and the Tabakin matrix elements are evaluated in the first and second order (Kerman and Pal 1967). In section 2, a brief description of the HF theory has been given together with the associated projection technique and the approximation scheme to the HF approach. Section 3 contains the details of the numerical calculations. In section 4, the excited states of ^{18}O in the TDA approach are explored. Section 5 contains the concluding remarks.

2. Theory

2.1. *Perturbation theory, HF scheme and projection*

The total Hamiltonian $\mathcal{H}$ is broken into two parts, the unperturbed Hamiltonian $\mathcal{H}_0 = T + V$ and the perturbation term $\mathcal{H}_1 = v - V$. T is the kinetic energy term, v the potential energy term and V some suitably defined single particle (s.p.) potential. The choice of the HF potential as the s.p. potential is very useful because it generates cancellation of many complicated terms in the perturbation expansion and ensures in general a rapid convergence of the series. The definition of the HF potential is given by

$$\langle \alpha \mid V \mid \beta \rangle = \sum_{\lambda=1}^{A} \langle \alpha\lambda \mid v \mid \beta\lambda \rangle \qquad (1)$$

where $\mid \lambda \rangle$ stands for the occupied states of the unperturbed system. The matrix elements are antisymmetric. Fuller details on the Rayleigh-Schrödinger perturbation theory and the HF approximation are already available in the literature (Day 1967, Ripka 1968). For singular potentials or for potentials having a strong short range repulsion, the general prescription is to replace v by the Brueckner reaction matrix t in equation (1) (one should be careful to use only the "on-energy shell" matrix elements in this definition).

The HF single-particle Hamiltonian is not necessarily invariant under all the symmetry operations that keep the total Hamiltonian invariant. If the intrinsic

HF wavefunction contains axial symmetry, states of good angular momentum are to be projected out to calculate physically meaningful quantities. The necessary formulae for energy, B(E2) rates, or quadrupole moments in projected states are given extensively in the literature (*see* for example, Ripka 1968).

2.2. *Approximation scheme to* HF *theory*

Let $|\Phi_0\rangle$ be the determinantal ground state of ^{18}O comprising the s.p. orbitals $|\alpha\rangle$, $|\beta\rangle$, etc. (figure 2)

$$|\Phi_0\rangle = \det(a, \beta, \ldots, \tilde{\alpha}\tilde{\beta}) \tag{2}$$

$|\alpha\rangle$, $|\beta\rangle$, etc. are the core states of the 0s and 0p shells. $|\tilde{\alpha}\rangle$, $|\tilde{\beta}\rangle$ are the states occupied by the two valence nucleons in the (1s-0d) shell, $|\tilde{\alpha}'\rangle$ etc. are unoccupied states in the (1s-0d) shell and $|a\rangle$'s are the states above the (1s-0d) shell. In the present calculation, these states are confined to the (1p-0f) shell. All these unpolarised states are the solutions of a Nilsson type Hamiltonian, *i.e.*, each of them arises from mixing of single-particle states in one major shell. Excitation of particles from the core states $|\alpha\rangle$ to the unoccupied states $|a\rangle$ causes a mixing among these states thereby polarising the core states. The polarised single-particle core orbital is then written as

$$|\alpha_P\rangle = |\alpha\rangle + \sum_a \langle a|f|\alpha\rangle |a\rangle \tag{3}$$

where f is a one body operator exciting nucleons from core states to the particle states. Polarisation of valence states is considered to be unimportant and is not taken into account.

The polarised determinant for the interacting system can then be written as

$$|\Phi_P\rangle = \det(\alpha_P, \beta_P, \ldots ; \tilde{\alpha}\tilde{\beta}) \tag{4}$$

$$= e^F |\Phi_0\rangle \tag{5}$$

where F is the operator defined as

$$F = \sum_{a,\alpha} \langle a|f|\alpha\rangle C_a^\dagger C_\alpha \tag{6}$$

Corresponding to the unpolarised and polarised s.p. states, we define the HF Hamiltonians h and h_P respectively, in the usual way,

$$h = T + V \tag{7 a}$$

$$h_P = T + V_P \tag{7 b}$$

and

$$\langle A|V|B\rangle = \sum_\alpha \langle A\alpha|v|B\alpha\rangle + \sum_{\tilde{\alpha}} \langle A\tilde{\alpha}|v|B\tilde{\alpha}\rangle \tag{8 a}$$

$$\langle A|V_P|B\rangle = \sum_\alpha \langle A\alpha_P|v|B\alpha_P\rangle + \sum_{\tilde{\alpha}} \langle A\tilde{\alpha}|v|B\tilde{\alpha}\rangle \tag{8 b}$$

A and B are any two arbitrary s.p. states and v is the two-nucleon "effective" potential. Substituting (3) in (8 b), we obtain, neglecting higher order terms in the excitation amplitudes,

$$\langle A \mid V_1 \mid B \rangle = \langle A \mid V \mid B \rangle + \sum_{a,\alpha} [\langle a \mid f \mid \alpha \rangle \langle A\alpha \mid v \mid Ba \rangle + \langle a \mid f^\dagger \mid \alpha \rangle \langle A\alpha \mid v \mid B\alpha \rangle] \tag{9}$$

We now introduce in (9) an approximate expression for the matrix elements of f, determined in the first order of approximation by looking upon h_0 as the result of a small perturbation over an unperturbed s.p. Hamiltonian based on h. Then

$$\langle a \mid f \mid \alpha \rangle = \frac{\langle a \mid h_1 \mid \alpha \rangle}{\epsilon_\alpha - \epsilon_a} \tag{10}$$

where h_1 is the perturbation term contained in h_0 and ϵ_α's are the eigenvalues of the unperturbed Hamiltonian. Since h as defined in (7 *a*) and (8 *a*) can produce a nonvanishing matrix element connecting $\langle a \mid$ and $\mid \alpha \rangle$, the unperturbed Hamiltonian is not h itself, but a part of h that is diagonal within the limited subspace of the individual major shells. There is a part in h that connects states like $\langle a \mid$ and $\mid \alpha \rangle$, *i.e.* states belonging to different major shells, and that has to be included in the definition of h_1. To make the statements explicit, we split h in the aforesaid "diagonal" and "nondiagonal" components,

$$h = h_0 + h_{ND} \tag{11}$$

and then write

$$h_0 = h - V_0 = V - h_{ND} + h_1 \tag{12}$$

where

$$h_1 = h_{ND} + V_0 - V \tag{13}$$

Substituting this expression for h_1 in (10), we finally obtain

$$\langle a \mid f \mid \alpha \rangle = \frac{\langle a \mid h_{ND} + V_0 - V \mid \alpha \rangle}{\epsilon_\alpha - \epsilon_a} + \frac{\langle a \mid h_0 + h_{ND} + V_0 - V \mid \alpha \rangle}{\epsilon_\alpha - \epsilon_a} + \frac{\langle a \mid h_0 \mid \alpha \rangle}{\epsilon_\alpha - \epsilon_a} \tag{14}$$

or

$$(\epsilon_\alpha - \epsilon_a) \langle a \mid f \mid \alpha \rangle + \sum_{c,\gamma} [\langle \gamma \mid f^\dagger \mid c \rangle \langle ac \mid v \mid a\gamma \rangle + \langle c \mid f \mid \gamma \rangle \langle a\gamma \mid v \mid ac \rangle] = - \langle a \mid h \mid \alpha \rangle \tag{15}$$

Equation (15) and its conjugate can be written in the matrix form,

$$\mathbf{M} \begin{pmatrix} f \\ g \end{pmatrix} = - \begin{pmatrix} h \\ -\tilde{h} \end{pmatrix} \tag{16}$$

where

$$f_{a\alpha} = \langle a \mid f \mid \alpha \rangle, \qquad g_{a\alpha} = \langle a \mid f^\dagger \mid \alpha \rangle,$$

$$h_{a\alpha} = \langle a \mid h \mid \alpha \rangle, \qquad \tilde{h}_{a\alpha} = \langle \alpha \mid h \mid a \rangle.$$

The matrix **M** is the well-known RPA matrix,

$$\mathbf{M} = \begin{pmatrix} A & B \\ -B & -A \end{pmatrix} \tag{17}$$

where

$$A_{a\alpha,\, c\gamma} = (\epsilon_a - \epsilon_\alpha)\, \delta_{ac}\, \delta_{\gamma\alpha} + \langle c\alpha \mid v \mid \gamma a\rangle$$
$$B_{a\alpha,\, c\gamma} = \langle ca \mid v \mid \gamma\alpha\rangle \tag{18}$$

The unknown amplitudes f and g can then be solved by matrix inversion,

$$\begin{pmatrix} f \\ g \end{pmatrix} = -\mathbf{M}^{-1} \begin{pmatrix} h \\ -\tilde{h} \end{pmatrix} = -\sum_i \frac{1}{|\omega_i|} \begin{pmatrix} x_i \\ y_i \end{pmatrix} (x_i^* - y_i^*) \begin{pmatrix} h \\ -\tilde{h} \end{pmatrix} \tag{19}$$

ω_i's are the eigenvalues of the RPA matrix and x_i, y_i's are the corresponding eigenvectors. $\sum_i \begin{pmatrix} x_i \\ y_i \end{pmatrix} (x_i^* - y_i^*)$ is the complete set of states corresponding to the non-Hermitian matrix **M**.

Once the s.p. polarised states are determined, states of good angular momentum are projected out from the polarised determinant,

$$E_J^P = \frac{\langle \Phi_P \mid \mathcal{H} P_J \mid \Phi_P\rangle}{\langle \Phi_P \mid P_J \mid \Phi_P\rangle} \tag{20}$$

P_J is the projection operator. Now,

$$\langle \Phi_P \mid P_J \mid \Phi_P\rangle = \langle \Phi_0 \mid e^{F\dagger} P_J e^F \mid \Phi_0\rangle$$
$$= \langle \Phi_0 \mid (1 + F^\dagger + \ldots) P_J (1 + F + \ldots) \mid \Phi_0\rangle \tag{21}$$
$$\langle \Phi_0 \mid P_J F \mid \Phi_0\rangle = \sum_{a,\, \alpha} \langle a \mid f \mid \alpha\rangle \langle \Phi_0 \mid P_J \mid \Phi_{a\alpha}\rangle$$

where

$$\mid \Phi_{a\alpha}\rangle = c_a^\dagger\, c_\alpha \mid \Phi_0\rangle$$

The action of P_J on $|\Phi_{a\alpha}\rangle$ is simply to rotate its s.p. states. If the unpolarised s.p. states are solutions of h_0 which does not allow major shell mixing, the rotated $|a\rangle$ state cannot be connected to any s.p. state comprising $|\Phi_0\rangle$. Consequently rotated $|\Phi_{a\alpha}\rangle$ has a vanishing overlap with $|\Phi_0\rangle$ and so

$$\langle \Phi_0 \mid P_J F \mid \Phi_0\rangle = \langle \Phi_0 \mid F^\dagger P_J \mid \Phi_0\rangle = 0 \tag{22}$$

when terms of second order in F are ignored (justified when f and g are small),

$$\langle \Phi_P \mid P_J \mid \Phi_P\rangle = \langle \Phi_0 \mid P_J \mid \Phi_0\rangle \tag{23}$$

Following the same type of argument, the numerator of (20) reduces to

$$\langle \Phi_P \mid \mathcal{H} P_J \mid \Phi_P\rangle = \langle \Phi_0 \mid \mathcal{H} P_J \mid \Phi_0\rangle$$
$$+ \sum_{a,\, \alpha} [\langle a \mid f \mid \alpha\rangle \langle \Phi_0 \mid \mathcal{H} P_J \mid \Phi_{a\alpha}\rangle + \langle \alpha \mid f^\dagger \mid a\rangle \langle \Phi_{a\alpha} \mid \mathcal{H} P_J \mid \Phi_0\rangle] \tag{24}$$

Then

$$E_J^P = \frac{\langle \Phi_0 \mid \mathcal{H} P_J \mid \Phi_0\rangle}{\langle \Phi_0 \mid P_J \mid \Phi_0\rangle} +$$

$$+\frac{\sum_{a,\alpha}[\langle a\,|f|\,a\rangle\langle\Phi_0\,|\,\mathcal{H}P_J\,|\,\Phi_{a\alpha}\rangle+\langle a\,|f^\dagger|\,a\rangle\langle\Phi_{a\alpha}\,|\,\mathcal{H}P_J\,|\,\Phi_0\rangle]}{\langle\Phi_0\,|\,P_J\,|\,\Phi_0\rangle}$$

$$=E_J+\mathscr{E}_J^P \tag{25}$$

E_J, the first term of (25), is the projected energy from the unpolarised Slater determinant and $\mathscr{E}_J^P$ is the polarisation correction. Since f and g are already known from (19), this correction term can be easily evaluated. Because of the very nature of the problem (two nucleons outside a closed shell) $\langle\Phi_0\,|\,\mathcal{H}P_J\,|\,\Phi_0\rangle$ can be easily evaluated through simple decoupling and recoupling of angular momenta. The final formulae are given in Appendix 1.

2.3. *Choice of the unperturbed s.p. Hamiltonian*

In the derivation given above, we have used the HF definition for the unperturbed s.p. Hamiltonian and have proposed to determine the s.p. unperturbed states through HF calculations in individual major shells. In actual computations, we have followed an approximate procedure by taking the unperturbed s.p. states from the solution of a Nilsson Hamiltonian confined to single major shells. In the usual way, the Nilsson Hamiltonian is defined by (Nilsson *et al* 1969)

$$h_N=T+\tfrac{1}{2}m\omega_0^2(\delta)\,r^2-\tfrac{4}{3}\sqrt{\pi/5}\,\delta\hbar\omega_0(\delta)f(\delta)\rho^2\,Y_0^2$$
$$-2k\hbar\omega_0^0\,\boldsymbol{l}.\boldsymbol{s}+2k\mu\hbar\omega_0^0(\rho^4-\langle\rho^4\rangle_N). \tag{26}$$

T is the kinetic energy operator, δ is the deformation parameter and ρ is the dimensionless spatial coordinate. $\rho=r/b$, b being the oscillator constant, $b=\sqrt{\hbar/m\omega_0^0}$.

$$\omega_0(\delta)=\omega_0^0 f(\delta)$$
$$f(\delta)=(1-4/3\delta^2-16/27\delta^3)^{-1/6}.$$

The strength parameters k and μ are chosen to be

$$k_n=0{\cdot}0641-0{\cdot}0026\times10^{-3}A,\qquad k_p=0{\cdot}0766-0{\cdot}0799\times10^{-3}A$$
$$\mu_n=0{\cdot}624-1{\cdot}234\times10^{-3}A,\qquad \mu_p=0{\cdot}493+0{\cdot}649\times10^{-3}A. \tag{27}$$

A is the nucleon number.

3. Numerical Results

3.1. *Intrinsic properties*

The s.p. orbitals are expanded in the spherical harmonic oscillator basis. In the initial calculation, the basis is truncated after the (1s-0d) shell. It is later extended to the (1p-0f) shell to study the improvement of the HF wavefunction and to study deformation and core-polarisation effects. Both the Coulomb interaction and the centre of mass (CM) correction have been ignored. The relative matrix elements are calculated with the oscillator energy parameter equal to 14 MeV.

The s.p. spectra for the Tabakin and the Hamada-Johnston (H-J) potentials are presented in table 1. The orbitals are found to be more bound for the Tabakin potential than for the H-J potential. The calculation in the smaller model space produces about 6·0 MeV spin-orbit splitting for the occupied p-states for both the potentials in close agreement with the experimental value (Tyren *et al* 1966),

Table 1. The single-particle energies (MeV)

	Max. Component			$0s_{1/2}^{1/2}$	$0p_{3/2}^{1/2}$	$0p_{3/2}^{3/2}$	$0p_{1/2}^{1/2}$	$0d_{5/2}^{1/2}$
Smaller Model Space	Tabakin		*n*	−54·232	−25·453	−24·306	−19·111	−3·646
			p	−56·521	−28·916	−25·764	−20·945	−8·113
	HJ		*n*	−48·457	−22·486	−21·309	−16·051	−1·308
			p	−50·326	−24·664	−21·898	−19·308	−2·128
Extended Model Space	Tabakin		*n*	−66·619	−33·325	−31·941	−23·275	−4·816
			p	−68·836	−36·679	−33·591	−25·280	−9·053
	HJ		*n*	−60·854	−30·629	−28·828	−20·717	−4·422
			p	−62·305	−32·685	−29·332	−21·996	−7·983
	Max. Component			$0d_{5/2}^{3/2}$	$0d_{5/2}^{5/2}$	$1s_{1/2}^{1/2}$	$0d_{3/2}^{1/2}$	$0d_{3/2}^{3/2}$
Smaller Model Space	Tabakin		*n*	−3·267	−2·457	−1·471	3·127	4·428
			p	−5·048	−3·406	−2·862	1·163	3·389
	HJ		*n*	−1·725	−0·949	−2·505	4·371	5·707
			p	−2·896	−1·207	−6·018	2·692	5·016
Extended Model Space	Tabakin		*n*	−4·078	−2·964	−0·993	4·476	6·029
			p	−5·876	−3·988	−2·509	2·477	4·904
	HJ		*n*	−3·369	−2·046	−2·063	4·630	6·375
			p	−4·475	−2·241	−2·781	2·906	5·719

6·60 MeV, for ^{16}O. Extension of the model space increases this splitting, and also pushes down the s.p. states, particularly the $0s_{\frac{1}{2}}$ state.

The binding energy per particle for the Tabakin potential is calculated to be 6·876 MeV in the extended basis, the corresponding quantity for the H-J potential being 5·067 MeV. The binding energies in the (1s-0d) basis are 5·666 MeV and 3·812 MeV for the Tabakin and the HJ interactions respectively. These values are quite lower in magnitude than the experimental value of $\sim$ 7·5 MeV. This inadequacy of the HJ and the Tabakin potential is by now quite well known.

A few definitions will now be made for an understanding of some relevant informations provided by the HF wavefunction. If a particular harmonic oscillator state is corrected by the mixture of another state differing only by the nodal quantum number, the correction would be called radial correction since this type of mixture determines the radial distribution of the wavefunction; the correction arising from mixing between states in the same major shell would be called deformation correction, and the mixture between states of different major shells (barring radial mixtures) would be called core-polarisation correction. Our HF results show that the main correction arising out of the extension of the model space is the radial correction. The deformation correction is small, and the core-polarisation correction is smaller. Tables 2 and 3 illustrate this point.

Table 2. Tabakin neutron HF wavefunctions in smaller model space.

	k	π	$0s_{1/2}$	$0p_{3/2}$	$0p_{1/2}$	$0d_{5/2}$	$1s_{1/2}$	$0d_{3/2}$
Occupied States	1/2	+	0·98393			0·01395	0·17743	0·01430
	1/2			0·98138	0·19210			
	3/2			1·0				
	1/2			0·19210	0·98138			
	1/2		0·05202			0·91291	0·37114	0·13037
Unoccupied States	3/2					0·99555		0·09423
	5/2					1·0		
	1/2		0·16663			0·38771	0·90135	0·09736
	1/2		0·04783			0·08323	0·13542	0·98657
	3/2					0·09423		0·99555

Table 3. Tabakin neutron wavefunctions in extended model space.

	k	π	$0s_{1/2}$	$0p_{3/2}$	$0p_{1/2}$	$0d_{5/2}$	$1s_{1/2}$
Occupied States	1/2	+	0·98606			0·01433	0·25407
	1/2			0·34612	0·15175		
	3/2			0·95602			
	1/2			0·14808	0·95955		
	1/2		0·06894			−0·93635	0·32241
Unoccupied States	3/2					0·99581	
	5/2					1·0	
	1/2		0·23968			0·34314	0·90012
	1/2		0·05281			0·07282	0·14588
	3/2					0·09149	

	k	π	$0d_{3/2}$	$0f_{7/2}$	$1p_{3/2}$	$0f_{5/2}$	$1p_{1/2}$
Occupied States	1/2	−	0·01527				
	1/2			0·01746	0·28131	0·01719	0·03097
	3/2			0·01498	0·29270	0·01159	
	1/2			0·00219	0·04680	0·02828	0·23310
	1/2		0·12068				
Unoccupied States	3/2		0·09149				
	5/2						
	1/2		0·12077				
	1/2	+	0·98520				
	3/2		0·99581				

The static mass and electric quadrupole moment, the r.m.s. radius and the energy gap between the occupied and unoccupied single-particle states are listed in table 4.

3.2. *Projected energies and electromagnetic properties*

The 0^+, 2^+, 4^+ levels projected from the HF wavefunction calculated in the smaller basis looks very compressed. Multishell projection improves the situation considerably, but no good agreement is yet obtained. Figure 3 demonstrates these statements for the Tabakin potential.

The electromagnetic properties of the nucleus, particularly the $B(E2)$ transition rates and the quadrupole moments in excited states have also been studied for the states projected from the HF wavefunction in the extended basis. It is seen that an

Table 4. The intrinsic quadrupole moments (Q), r.m.s. radii (R) and HF energy-gap. Experimental r.m.s. radius = 2·55 fm [value of r_0 has been taken from Preston (1965)]

	Neutron Q (fm^2)	Proton Q (fm^2)	Total Q (fm^2)	Neutron R (fm)	Proton R (fm)	Total R (fm)	HF energy-gap (MeV)
Tabakin (p—f)	5·064	0·636	5·699	2·542	2·332	2·451	0·739
Tabakin (s—d)	4·956	0·129	5·085	2·788	2·658	2·731	0·380
HJ (p—f)	5·889	0·693	6·583	2·549	2·331	2·455	1·053
HJ (s—d)	5·095	0·112	5·207	2·804	2·654	2·739	0·780

effective charge of 1·5e for protons and 0·5e for neutrons reproduces the experimental data nicely. The values of the effective charge parameters are consistent with earlier calculation (Halbert *et al* 1971) in this region. The projection results are summarised in table 5. The 4^+ states in the HJ projected spectrum in both the model spaces go too high in energy. This strongly suggests the presence of a big and repulsive hexadecapole component in the HJ potential.

3.3. *Pairing corrections*

Pairing corrections to the HF ground state have been treated by the method described by Pal and Stamp (1967) which considers excitation of a pair of nucleons from a pair of time-reversed occupied states to a similar pair of states above the Fermi-sea. Preliminary computations of the excitation amplitudes by the first-order perturbation formula confirmed that only the excitation from the last occupied neutron-orbit ($\frac{1}{2}^+$) and its degenerate time-reversed partner ($-\frac{1}{2}^+$) to the five similar unoccupied pair states in the s-d shell is important. Results for the energy levels, obtained by angular momentum projection from the correlated ground state (the HF state plus the correction due to pair excitation) are presented in table 6, and figure 3. The $0^+ - 2^+$ separation shows a further improvement towards the experimental data.

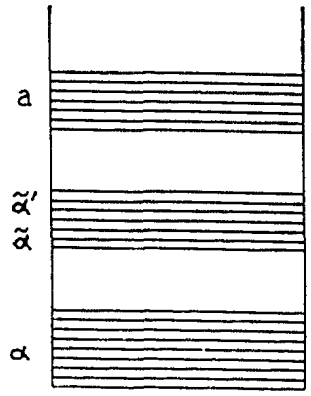

Figure 2. The unperturbed single-particle orbitals used in the approximation scheme to HF theory.

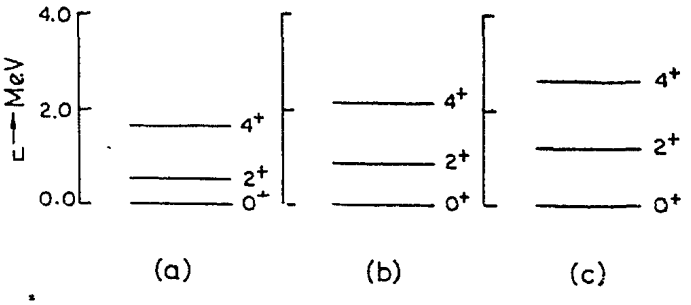

Figure 3. The projected spectrum for the Tabakin potential. The gradual improvement from the smaller model space to the extended model space followed by pair correlation has been demonstrated [(*a*) (1s–0d), (*b*) (1p–0f), (*c*) (1p–0f) and correlations].

Table 5. The level spacing, B (E2) rates and quadrupole moments (Q) with effective charge for protons $= 1{\cdot}5\,e$, and for neutrons $= 0{\cdot}5e$

	0^+-2^+ Separation (MeV)	2^+-4^+ Separation (MeV)	$B(E2)(2^+-0^+)$ e^2fm^4	$B(E2)(4^+-2^+)$ e^2fm^4	$Q(2^+)$ fm^2	$Q(4^+)$ fm^2
Tabakin (p–f)	0·879	1·291	6·48	7·15	−2·38	−3·64
Tabakin (s–d)	0·544	1·139				
HJ (p–f)	1·004	3·076	8·12	9·88	−3·01	−4·04
HJ (s–d)	0·839	2·380				
Expt.	1·98	1·57	7·5±1·4	⩽12·1		

Table 6. Projection results from the correlated ground state. All energies are in MeV

	Energy Sep. (MeV)		
	Tabakin (s–d)	Tabakin (p–f)	Expt.
Levels			
0^+-2^+	1·074	1·204	1·98
2^+-4^+	1·364	1·408	1·57

Because only the excitation of the last neutron pair is important, only the $T = 1$ pairing concerns us here. A more general pairing with also the $T = 0$ interaction (Padjen and Ripka 1970) causes insignificant change in the particular case of ^{18}O. This point has been checked by detailed computations.

The strength of the HF state in the correlated ground state is found to be nearly 85 per cent and charges very little with the inclusion of more pair excited states. However, when the computation is done in the restricted (*i.e.* up to the 1s-0d shell) basis, the strength of the HF state is only about 45 per cent and it improves to nearly 70 per cent with the inclusion of the full set of pair-excitations. This merely shows the instability of the HF solution in the smaller model space, while in the larger space the inclusion of the 0f-1p shell gives the required stability.

3.4. *Results by the approximate method*

The Nilsson Hamiltonian (expression 26) is diagonalised in the spherical harmonic oscillator basis in single major shells. The oscillator energy parameter is chosen to be $\hbar\omega_0{}^0 = 38A^{-1/3}$ MeV for protons and equal to $44A^{-1/3}$ MeV for neutrons.

The expectation value $\langle h_N \rangle$ shows a minimum for the deformation parameter δ equal to 0·175. The entire calculation is done with the s.p. wavefunctions and energies corresponding to this value of the deformation. The states $|a\rangle$ (figure 2) are confined within the (1p-0f)-shell and the states $|\alpha\rangle$ are confined within the (0p)-shell. The eigenvalues and eigenvectors of the RPA-matrix (expressions (17)

Table 7. Nilsson projection results and polarisation corrections. All energies are in MeV.

	Nilsson		Polarisation Correction		Total		HF (p − f)	
Levels	Tabakin	H–J	Tabakin	H–J	Tabakin	H–J	Tabakin	H–J
0^+	−98·325	−65·168	−17·736	−11·292	−116·061	−76·460	−124·855	−92·455
2^+	−97·456	−64·201	−17·712	−11·396	−115·168	−75·597	−123·978	−91·451
4^+	−96·082	−62·134	−17·528	−11·028	−113·610	−73·162	−122·684	−88·375

Table 8. Projected results after adjustment of two-body matrix elements. The energies are in MeV

	Nilsson		Polarisation Correction		Total	
Levels	Tabakin	H–J	Tabakin	H–J	Tabakin	H–J
0^+	−83·913	−47·640	−4·689	−3·035	−88·602	−50·675
2^+	−81·918	−45·716	−4·639	−3·036	−86·557	−48·752
4^+	−80·380	−44·084	−4·642	−3·049	−85·022	−47·133

and (18)) have been obtained by the procedure described in Appendix 2. The positive energy eigenvectors are normalised by requiring $\Sigma_i\ (x_i^2 - y_i^2) = 1$.

The excitation amplitudes f and g are obtained from equation (19). The smallness of the calculated values of f and g confirms that the approximation of treating the model Nilsson Hamiltonian as the unperturbed Hamiltonian is very good and consequently, the omission of higher order terms in f and g is justified.

Good angular momentum states have been projected out from the Nilsson determinant. The resulting spectrum is more stretched than the one obtained from the HF determinant, the model space remaining the same. Polarisation corrections after inclusion of states outside the model space are then evaluated from eq. (25). The Nilsson projection results and the polarsiation corrections are presented in table 7. For both the potentials, binding energy obtained from the Nilsson determinant is nearly 5 MeV less than that obtained from the HF wavefunction computed in the smaller model space. The polarisation gain in energy is nearly J-independent. It is nearly 17·7 MeV for the Tabakin potential and nearly 11 3 MeV for the HJ potential. The spectrum, even after the polarisation correction has been included, does not give a good fit to the energy level data. Core polarisation in the HF calculation gives a gain in the binding energy $\sim$ 22 MeV for both the potentials. In the approximate calculations, the core polarisation gain in the binding energy is somewhat smaller. The total binding energy after the core polarisation correction is nearly 9 MeV less for the Tabakin potential and nearly 16 MeV less for the HJ potential than that obtained from multi-shell HF calculation. This is because of the neglect of the polarisation correction of the (0s)-nucleons of the core.

It has been found that the spectra can be reproduced accurately by arbitrarily multiplying the $J = 0$ and 2 matrix elements ($T = 1$) for the Tabakin potential by 1·4 and 0·6 respectively. For the Hamada-Johnston potential we also needed a change in the $J = 4$, $T = 1$ matrix element by a factor of 1·2. The total binding energy of the nucleus then decreases by an appreciable amount (~12 MeV) and it is found that the binding energy is quite sensitive to the $J = 2$, $T = 1$ matrix elements, but quite insensitive to the $J = 4$, $T = 1$ matrix elements. The Nilsson projection results and the polarisation corrections with the changed matrix elements, as described above, are presented in table 8. The amplitudes f and g decrease by about 50% and the core polarisation corrections by about 75%. But the independence of the core polarisation corrections on the J-values is demonstrated again. If the change in the two-body matrix elements could have reproduced the binding energy properly, it would have been more interesting, but it is found that one cannot be done without some sacrifice to the other.

4. The excited bands

Besides the 0^+, 2^+, 4^+ states so far dealt with, the experimental spectrum of ^{18}O shows several other states. A programme for an understanding of the origin of these states was also undertaken. To generate excited bands built upon the original HF solution, the Tamm-Dancoff Approximation (TDA) was used. Ground state correlations have been neglected for simplicity.

The calculations have been limited to the (1s-0d) model space to reduce the computational labour. Since the s.p. states have axial symmetry, the Tamm-Dancoff calculation yields excited bands having a definite band quantum number. For the generation of excited positive parity bands, excitations from the last two occupied neutron orbitals to the unoccupied neutron orbitals in the (1s-0d) shell has only been considered and the other neutron and proton excitations, namely excitation from the 0s-shell has been neglected. The $K = 0$ excited band arises from the superposition of four particle-hole determinants, the $K = 1$ from four, the $K = 2$ from three and the $K = 3$ band is a single determinant. Calculations with the Tabakin matrix elements yield the band heads of the above bands at 2·24,

Table 9. The projected energy values from different bands. The results are in MeV. The ground state energies ($J=0^+$) are −102·682 (Tabakin) and −69·744 MeV (HJ) respectively.

	$K = 0$ band		$K = 1$ band		$K = 2$ band		$K = 3$ band	
	E_J (Tab.)	E_J (HJ)	E_J (Tab.)	E_J (HJ)	E_J (Tab.)	E_J (HJ)	E_J (Tab.)	E_J (HJ)
0^+	−100·760	−67·805						
1^+			− 92·217	−58·677				
2^+	−99·017	−67·316	−101·795	−68·707	−99·008	−67·259		
3^+			− 99·011	−66·104	−98·930	−66·245	−98·637	−66·399
4^+	−97·504	−64·880	−101·197	−65·249	−96·746	−63·266	−97·982	−65·746

Table 10. The energy eigenvalues after bandmixing (in MeV) and the bandmixing amplitudes. The results are for the Tabakin interaction.

J	E_J	$K=0$	$K=1$	$K=2$	$K=3$
0^+	−100·760	1·0			
1^+	− 92·217		1·0		
2^+	−100·611	0·69782	0·49176	−0·52077	
2^+	− 99·963	0·81348	0·00916	0·58151	
2^+	− 85·633	0·62344	0·70634	−0·33525	
3^+	− 99·433		0·60879	−0·71052	−0·35288
3^+	− 92·560		0·74576	0·66044	0·08746
3^+	− 87·132		0·60020	−0·18234	0·77878
4^+	− 98·555	0·74730	0·58777	−0·05482	−0·30505
4^+	− 92·406	0·60037	0·68978	−0·30555	0·26530
4^+	− 90·117	0·28250	−0·04063	0·92467	−0·25204
4^+	− 89·985	0·34959	−0·08669	−0·39813	0·84365

0·83, 1·39 and 1·71 MeV respectively above the HF energy. The same energies for the HJ potential are 1·36, 1·25, 1·98 and 2·23 MeV.

States of good angular momenta are projected out from the intrinsic band wave functions. The results are given in table 9. There are one 0^+, three 2^+, three 3^+ and four 4^+ states, all crowded in a narrow energy interval of about 4 MeV. The 1^+ state projected from the $K=1$ band lies at about 10 MeV above the ground state. The result follows from calculations with both the interactions. This agrees with the observation that there is no 1^+ excitation at low energies.

Since the band heads and projected energies are very close to each other, band mixing is quite important and has been taken into account. The 0^+ and 1^+ states are pure projected states from the $K=0$ and $K=1$ bands and their positions remain unchanged. The $K=0$, $K=1$ and $K=2$ bands mix for the determination of the 2^+ states, the $K=1$, $K=2$ and $K=3$ bands mix for determining the position of the 3^+ states, and for the determination of the 4^+ states all the four bands mix. When band mixing is taken into account, the Schrödinger equation

$$\mathcal{H}\psi_M^J = E\psi_M^J$$

transforms to

$$\mathcal{H}a = E\mathbf{O}a \tag{28}$$

where a is the eigenvector, and $\mathbf{O}$ is the overlap matrix, any matrix element of which is the overlap between states of same J and $\mathbf{M}$ projected from states of different or the same band.

If we choose

$$b = \mathbf{O}^{\frac{1}{2}} a \tag{29}$$

equation 28 reduces to

$$\mathbf{O}^{-\frac{1}{2}}\mathcal{H}\mathbf{O}^{\frac{1}{2}} b = Eb \tag{30}$$

Table 11. The energy eigenvalues after bandmixing (in MeV) and the bandmixing amplitudes. The results are for the HJ interaction.

J	E_J	$K=0$	$K=1$	$K=2$	$K=3$
0^+	−67·805	1·0			
1^+	−58·677		1·0		
2^+	−67·699	0·95646	0·21752	0·19459	
2^+	−66·803	−0·69260	−0·23876	0·68065	
2^+	−55·932	0·68309	0·61288	−0·39717	
3^+	−66·884		0·75773	0·11876	0·64166
3^+	−58·936		0·16851	−0·14748	0·97460
3^+	−52·135		0·57293	−0·22414	0·78835
4^+	−64·019	0·95461	0·25763	−0·04569	0·14232
4^+	−58·634	0·64354	0·76457	−0·03435	−0·00998
4^+	−56·591	0·25272	−0·13936	0·85049	−0·43973
4^+	−53·773	0·68637	0·22993	−0·17052	0·66853

Diagonalisation of the symmetric matrix $\mathbf{O}^{-\frac{1}{2}}\mathcal{H}\mathbf{O}^{-\frac{1}{2}}$ yeilds the desired eigenvalues. The eigenvectors a can then be obtained from equation (29). They give a measure of the bandmixing strengths.

The energies of different states, computed with band mixing, are presented in tables 10 and 11. The interesting feature of bandmixing is that one 2^+, two 3^+ and three 4^+ states are pulled up quite high in energy. This makes it easier to compare (figure 4) the calculated spectrum with the experimental one because as many states as are observed experimentally at low energies remain present in the calculated spectrum in that energy range. For the Tabakin interaction, the fit to the spectrum is quite fair when the whole excited band spectrum is pushed up a little as has been done in figure 4. For the HJ interaction, the general ordering of the indivdual states is maintained properly except for one observation that the 3^+ state lies a little below the second 2^+ of the excited spectrum. The 4^+ state shoots high up like the projected 4^+ state from the ground state band.

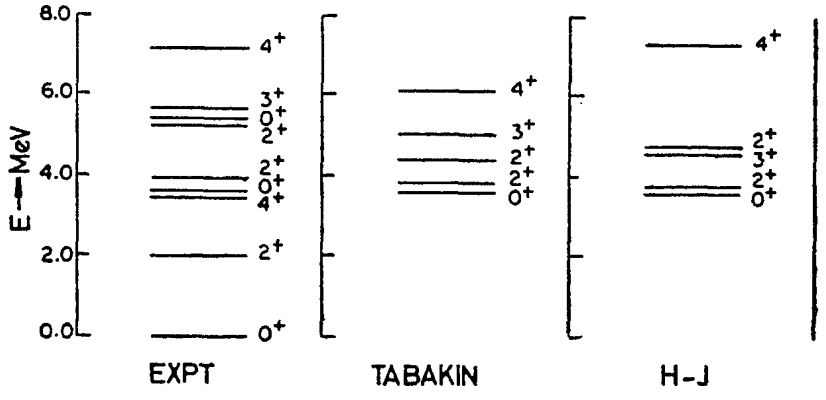

Figure 4. The projected spectrum from the excited bands with the inclusion of bandmixing. The figure has been drawn so that the first excited 0^+ of the computed spectra coincides with that of the experimental spectrum.

5. Concluding remarks

5.1. *On the numerical results*

There are several aspects of the numerical results, presented in this paper, which require elucidating comments. It is clear from the results that there is a systematic improvement in the (0^+, 2^+, 4^+) spectrum as one goes from the smaller to the extended basis, and then one further includes the effect of pairing. This is what is to be expected. The HF solution in the extended basis is more stable, produces a larger energy-gap between the occupied and unoccupied states, and hence decreases the moment of inertia. Similarly the effect of pairing in reducing the moment of inertia is quite well known and well understood.

The discrepansy in the spectrum that still remains has to be attributed partly to the deficiencies of the two-body matrix elements, and partly to the static nature of the HF computation. It is well known that fairly stable deformations in the (1s-0d) shell occur at ^{20}Ne and persist for several nuclei above it. The nucleus ^{18}O belongs to the transitional region leading to this region of deformation. Some amount of dynamics of the deformation will be needed in order to produce a complete agreement with the experimental spectrum in this nucleus. This dynamical effect will enhance the B(E2) transitions further and will bring them into closer agreement with the experimental values without the introduction of a high value of the effective charge that appears in table 5. Some preliminary results along this direction, obtained by one of us (M K P), confirm the above conjecture and will be published elsewhere.

The approximate method, as it is described in section 2 (and *not* with the Nilsson potential, which has been used here in actual computations), consists basically of starting with an approximate single-particle density matrix ρ_0, confined to single major shells, and then obtaining the first-order correction ρ_1 to it when RPA-type hole-particle excitations are allowed. By diagonalising the new ($\equiv \rho_0 + \rho_1$) and then using the eigenstates to define a new set of occupied states, one can repeat the process of generating the new correction ρ_1 to the new ρ, and so on. In principle, therefore, the approximate method described here is the first step of a new method of iteration towards the correct Hartree-Fock solution in an extended space, starting with a more limited space. This method of iteration is quite distinct from the conventional method of iteration emlopyed in obtaining the HF solution. It can be shown that, except in certain pathological cases, this new method of iteration guarantees faster convergence, and in that sense the first iteration, which has been described as the approximate method in this paper, is already very close to the correct HF solution. Schiffrer and Collaborators (1973) have been working in details on a method of fast convergence of the Hartree-Fock calculation, and the remarks on the convergence, made above, follow as a direct corollary to the proof by these workers.

The formulae of Appendix 1 reveal that, had the first two terms inside the square brackets in (A. 1.2) been small compared to the last term, then the core polarisation correction computed by the approximate method becomes nearly independent of J. Numerical results show that this is so. This is somewhat in contrast to what was found in the exact HF computation when the basis was extended. However, this discrepancy between the exact and the approximate computation can be

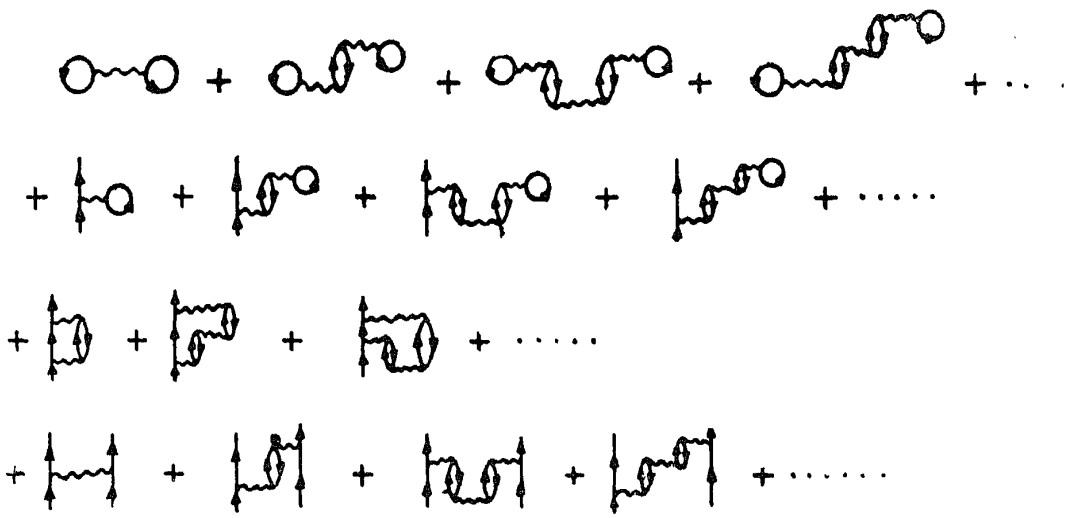

Figure 5. Diagrams that enter into the approximate HF calculation.

understood in the following way. As observed earlier, the spreading of the spectrum for the extended basis in the HF calculation is due to the extra stability acquired by the HF solution. By contrast, the Nilsson potential used in the approximate solution already produced a fairly stable solution with a larger energy gap. Therefore, when the density was improved by the RPA contribution to the ρ_1, the gain in the stability of the solution was not as spectacular as in the case of the HF calculation. Hence the moment of inertia remained more or less the same. Presumably, the results would have been different had the HF solutions restricted to major shells, been used instead of the Nilsson states in the approximate method.

5.2. *Comparison with the diagrams of the renormalised two-body potential*

In the shell model approach the interaction between valence nucleons is renormalised through selected higher order sums of diagrams in perturbation theory, the selected processes being 3p-1h, TDA and RPA type of core excitations, screening of the particle-hole (p-h) interaction and vertex renormalisation (figure 1). It has been mentioned in the introduction that when all these processes are summed up to all orders, the resulting spectrum is in poor agreement with the experimental levels.

In the present paper the HF approach has been used for the exploration of the spectral properties of ^{18}O. Results obtained with the multi-shell HF calculation has been compared with those using an approximate version of the HF theory. The latter has the agreeable feature of a close parallel with the diagrams of the shell-model approach, mentioned above. The diagrams that enter into the approximate calculations are shown in figure 5.

Let us now examine the role played by the different vertices of figure 1. The 3p-1h vertex is shown diagrammatically in figure 6 *a* and the corresponding HF diagram is shown in figure 6 *b*. In figure 6 *a* the vertical line represents a valence state and the diagram involves a matrix element of the type $\langle$1s-0d, 0p$|t|$1s-0d, 1p-0f$\rangle$. This means that the core state is being mixed with 1p-0f state and is thus being polarized. Such matrix elements enter in the multi-shell HF calculation in a very natural way. The HF procedure achieves one thing further, the positive parity core states as well as the valence states also get polarised. Referring to figure 6 *b*, we note that this diagram (summed over all occupied states including

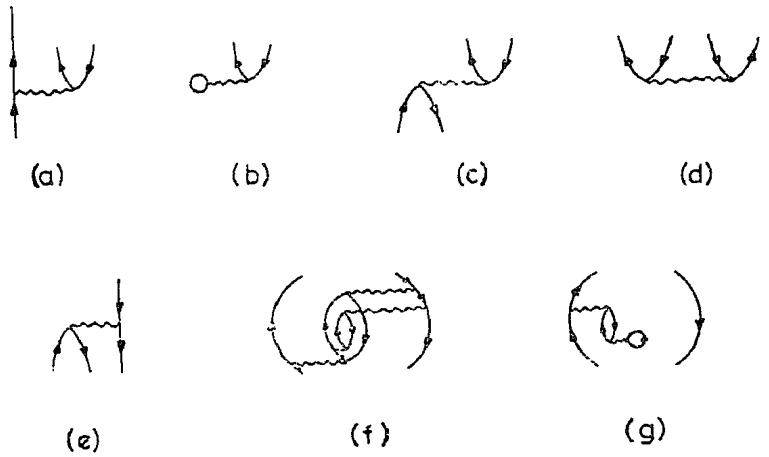

Figure 6. (*a*) The 3p–1h vertex; (*b*) The HF analogue of the 3p–1h vertex; (*c*) The TDA vertex; (*d*) The RPA vertex; (*e*) The self-screening vertex; (*f*) Diagrams that should have been included in self-screening; (*g*) The Pauli-violating self-screening diagram entering into the HF calculation.

the valence ones) equals zero when the p-h states are determined in the self-consistent manner. Thus not only that the daigram like figure 6 *a* is present in the HF calculation, the latter method also makes use of an exact cancellation of its contribution when summed with the same diagram for the remaining occupied states.

The TDA and RPA vertices are shown in figure 6 *c* and figure 6 *d*. The TDA vertex involves a matrix element of the type $\langle$1p-0f, 0p $|\, t \,|$ 0p, 1p-0f$\rangle$ and the RPA vertex involves a matrix element of the type $\langle$1p-0f, 1p-0f $|\, t \,|$ 0p, 0p$\rangle$. These matrix elements also enter into the HF calculation very naturally. The presence of these diagrams becomes more explicit in the approximate method described in this paper where the TDA and RPA modes of excitation of the core come as a natural consequence in the determination of the p-h excitation amplitudes.

The self-screening vertex is shown in figure 6 *e*. This vertex involves matrix elements of the type $\langle$0p, 0p $|\, t \,|$ 0p, 1p-0f$\rangle$. They are clearly present in the HF calculation in the determination of the negative parity s.p. energies and wavefunctions and diagonalisation of the HF Hamiltonian essentially means that the self-screening diagrams are present to all orders in our calculations.

In drawing the self-screening diagrams, a few cautions are worth keeping in mind. We must remember that nesting within the primary 3p-1h bubble cannot go to all orders. If n be the number of particles in the core available for excitation, the number of bubbles within the primary bubble cannot be more than $n-1$ and this restricts the nesting of the self-screening diagram to all orders. This restriction would reduce the effect of screening on the core polarisation to some extent. Furthermore, it is not at all apparent why diagrams of the type shown in figure 6 *f* should not be present in self-screening. The number of such diagrams would increase enormously as the number of secondary bubbles within the primary one increases and it is difficult to work out what role they would play in the complicated process of core polarisation.

Referring back to our Hartree-Fock procedure, the type of diagram shown in figure 6*g* enters in our calculation since the particle energy is the self-consistent energy. The particle is excited leaving a vacancy in the occupied states, but since

the presence of a bubble means the sum over all occupied states, this type of diagram has the inevitable effect of violation of the Pauli principle. It is clear that the nested self-screening diagram of the same order has the effect of compensation for that violation. It is thus difficult to understand why one particular set of diagrams correcting for the Pauli principle be given importance in the renormalisation of the two-body matrix elements. In the absence of a suitable expansion parameter, the summing of all such diagrams to all orders, however elegant the resultant equation may be, is likely to be an inconsistent and erroneous procedure.

The vertex modification graphs play a central role in damping the core-polarisation contribution. Most possibly, these graphs are not included in our multishell HF calculation.

Appendix 1

Since the unpolarised wave functions are Nilsson wavefunctions determined in single major shell diagonalisation, the ^{16}O core wavefunctions couple the total core angular momentum to zero. The ^{18}O determinant can then be represented as

$$| \Phi_0\rangle = c_i^\dagger \, c_j^\dagger \, | 0\rangle \tag{A. 1.1}$$

$| 0\rangle$ is the ^{16}O core determinant, $| i\rangle$ and $| j\rangle$ are the two valence nucleon states related to each other through time reversal symmetry. The sum of the projection quantum numbers of the valence states is then zero. When these states are expanded in spherical HO basis

$$| i\rangle = \sum_\eta x_\eta{}^i \, | \eta\rangle, \quad | j\rangle = \sum_\xi x_\xi{}^i \, | \xi\rangle,$$

$$\langle \Phi_0 \,|\, \mathcal{H} P_J \,|\, \Phi_{a a}\rangle = [1 + (-)^J] \sum_{\xi\eta} \begin{bmatrix} j_\xi & j_\eta & J \\ m_\xi & m_\eta & 0 \end{bmatrix}^2 \times$$

$$\times [\, | x_\xi{}^j |^2 \, x_\eta{}^{i*} \langle \alpha\eta \,|\, v \,|\, ai\rangle + | x_\xi{}^i |^2 \, x_\eta{}^{j*} \langle \alpha\eta \,|\, v \,|\, aj\rangle$$

$$+ | x_\xi{}^j |^2 \, | x_\eta{}^i |^2 \langle a \,|\, h_0 \,|\, \alpha\rangle] \tag{A. 1.2}$$

h_0 is the core s.p. operator defined as

$$\langle \alpha \,|\, h_0 \,|\, \beta\rangle = \langle \alpha \,|\, T \,|\, \beta\rangle + \sum_{\lambda=1}^{core} \langle \alpha\lambda \,|\, v \,|\, \beta\lambda\rangle \tag{A. 1.2}$$

$\langle \Phi_0 \,|\, \mathcal{H} P_J \,|\, \Phi_0\rangle$ and $\langle \Phi_0 \,|\, P_J \,|\, \Phi_0\rangle$ are evaluated following the same procedure.

$$\langle \Phi_0 \,|\, \mathcal{H} P_J \,|\, \Phi_0\rangle = [1 + (-)^J] \sum_{\xi\eta} \begin{bmatrix} j_\xi & j_\eta & J \\ m_\xi & m_\eta & 0 \end{bmatrix}^2 \times$$

$$\times [\, | x^j{}_\eta |^2 \, x^i{}_\xi \langle i \,|\, h_0 \,|\, \xi\rangle + | x_\xi{}^i |^2 \, x^j{}_\eta \langle j \,|\, h_0 \,|\, \eta\rangle + x_\xi{}^i \, x_\eta{}^j \langle ij \,|\, v \,|\, \xi\eta\rangle$$

$$+ | x_\xi{}^i |^2 \, | x_\eta{}^j |^2 \{ \sum_\alpha \langle \alpha \,|\, h_0 \,|\, \alpha\rangle - \tfrac{1}{2} \sum_{\alpha\beta} \langle \alpha\beta \,|\, v \,|\, \alpha\beta\rangle \}] \tag{A. 1.4}$$

$$\langle \Phi_0 \,|\, P_J \,|\, \Phi_0\rangle = [1 + (-)^J] \sum_{\xi\eta} \begin{bmatrix} j_\xi & j_\eta & J \\ m_\xi & m_\eta & 0 \end{bmatrix}^2 | x_\xi{}^i |^2 \, | x_\eta{}^j |^2 \tag{A. 1.5}$$

Appendix 2

The RPA equation is given by

$$\begin{pmatrix} A & B \\ -B & -A \end{pmatrix} \begin{pmatrix} X \\ Y \end{pmatrix} = E \begin{pmatrix} X \\ Y \end{pmatrix} \tag{A. 2.1}$$

Let $\Gamma = X + Y$ and $\triangle = X - Y$

then

$$\begin{pmatrix} A & B \\ -B & -A \end{pmatrix} \begin{pmatrix} \Gamma + \triangle \\ \Gamma - \triangle \end{pmatrix} = E \begin{pmatrix} \Gamma + \triangle \\ \Gamma - \triangle \end{pmatrix} \qquad \text{(A. 2.2)}$$

From (A. 2.2), we obtain

$$(A - B)\triangle = E\Gamma \qquad \text{(A. 2.3)}$$

and

$$(A + B)\Gamma = E\triangle \qquad \text{(A. 2.4)}$$

Substituting the value of $\triangle$ obtained from (A. 2.4) in (A. 2.3), we get,

$$(A - B)(A + B)\Gamma = E^2\Gamma \qquad \text{(A. 2.5)}$$

Thus diagonalisation of the matrix $(A - B)(A + B)$ gives the squares of the energy eigenvalues and the eigenvectors Γ. $\triangle$ is then obtained from (A. 2.4). These in turn give the eigenvectors X and Y.

References

Barrett B R and Kirson M W 1970 *Nucl. Phys.* **A148** 145

Bloch C and Horowitz J 1958 *Nucl. Phys.* **8** 91

Brueckner K A 1955 *Phys. Rev.* **97** 1353

Clement D M and Baranger E U 1968 *Nucl. Phys.* **A108** 27

Day B D 1967 *Rev. Mod. Phys.* **39** 719

Ellis P J and Siegel S 1970 *Nucl. Phys.* **A152** 547

Halbert E C, Mcgrory J B, Wildenthal B H and Pandya S P 1971 *Adv. Nucl. Phys.* **4** 316

Hamada T and Johnston I D 1962 *Nucl. Phys.* **34** 382

Kerman A and Pal M K 1967 *Phys. Rev.* **162** 970

Kirson M W ard Zamick L 1970 *Ann. Phys. (N.Y.)* **60** 188

Kirson M W 1971 *Ann. Phys. (N.Y.)* **66** 624

Kuo T T S and Brown G E 1966 *Nucl. Phys.* **85** 40

Kuo T T S 1967 *Nucl. Phys.* **A103** 71

Nilsson S G, Tsang C F, Sobiezewski A, Szymanski Z, Wyekti S, Gustafson C, Lamm I, Moller P and Nilsson B 1969 *Nucl. Phys.* **A131** 1

Osnes E, Kuo T T S and Warke C S 1971 *Nucl. Phys.* **A168** 190

Padjen R and Ripka G 1970 *Nucl. Phys.* **A149** 273

Pal M K and Stamp A P 1967 *Nucl. Phys.* **A99** 228

Preston M A 1965 *Physics of the nucleus* (Addison-Wesley Publishing Company, Inc., New York)

Ripka G 1968 *Adv. Nucl. Phys.* **1** 183

Schiffrer G Trieste Lectures, 1973

Tab kin F 1964 *Ann. Phys. (N.Y.)* **30** 51

Tyren H, Kullander S, Sundberg O, Ramachandran R, Isacsson P and Berggrey T 1966 *Nucl. Phys.* **79** 321